



**Queensland University of Technology**  
Brisbane Australia

This may be the author's version of a work that was submitted/accepted for publication in the following source:

Jian, Haigen, Luo, Jian, Ou, Ling, Tang, Xianmin, & Yan, Cheng  
(2017)

Micro-morphology of fatigue crack initiation and propagation behavior in high strength aluminum alloy.

*Materials Science & Engineering A: Structural Materials: Properties, Microstructure and Processing*, 684, pp. 213-221.

This file was downloaded from: <https://eprints.qut.edu.au/102284/>

**© Consult author(s) regarding copyright matters**

This work is covered by copyright. Unless the document is being made available under a Creative Commons Licence, you must assume that re-use is limited to personal use and that permission from the copyright owner must be obtained for all other uses. If the document is available under a Creative Commons License (or other specified license) then refer to the Licence for details of permitted re-use. It is a condition of access that users recognise and abide by the legal requirements associated with these rights. If you believe that this work infringes copyright please provide details by email to [qut.copyright@qut.edu.au](mailto:qut.copyright@qut.edu.au)

**License:** Creative Commons: Attribution-Noncommercial-No Derivative Works 2.5

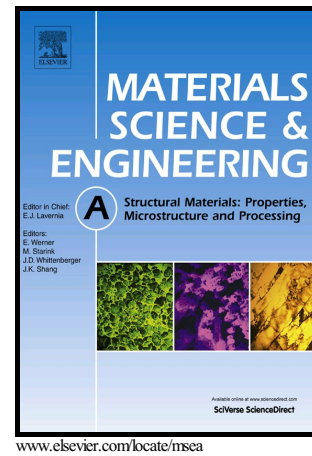
**Notice:** *Please note that this document may not be the Version of Record (i.e. published version) of the work. Author manuscript versions (as Submitted for peer review or as Accepted for publication after peer review) can be identified by an absence of publisher branding and/or typeset appearance. If there is any doubt, please refer to the published source.*

<https://doi.org/10.1016/j.msea.2016.11.046>

# Author's Accepted Manuscript

## Micro-morphology of Fatigue Crack Initiation and Propagation Behavior in High Strength Aluminum Alloy

Haigen Jian, Jian Luo, Ling Ou, Xianmin Tang, Cheng Yan



PII: S0921-5093(16)31401-0  
DOI: <http://dx.doi.org/10.1016/j.msea.2016.11.046>  
Reference: MSA34372

To appear in: *Materials Science & Engineering A*

Received date: 27 July 2016  
Revised date: 13 October 2016  
Accepted date: 12 November 2016

Cite this article as: Haigen Jian, Jian Luo, Ling Ou, Xianmin Tang and Cheng Yan, Micro-morphology of Fatigue Crack Initiation and Propagation Behavior in High Strength Aluminum Alloy, *Materials Science & Engineering A* <http://dx.doi.org/10.1016/j.msea.2016.11.046>

This is a PDF file of an unedited manuscript that has been accepted for publication. As a service to our customers we are providing this early version of the manuscript. The manuscript will undergo copyediting, typesetting, and a review of the resulting galley proof before it is published in its final citable form. Please note that during the production process errors may be discovered which could affect the content, and all legal disclaimers that apply to the journal pertain.

**Micro-morphology of Fatigue Crack Initiation and Propagation Behavior in High  
Strength Aluminum Alloy**

Haigen Jian<sup>1,2</sup>, Jian Luo<sup>1</sup>, Ling Ou<sup>1</sup>, Xianmin Tang<sup>1\*</sup>, Cheng Yan<sup>2</sup>

1. Hunan University of Technology, Zhuzhou 412007, China

2. Queensland University of Technology, Queensland 4001, Australia

\*Corresponding author. Tel: +86-13973386987; fax: +86-731-22183465. tangxianmin@hut.edu.cn

**Abstract**

The microscopic morphology of fatigue crack initiation and propagation behavior was investigated for B93T4 high strength aluminum using optical microscopy, scanning electron microscopy and transmission electron microscopy. The results show that, the fatigue micro-crack generally initiates on the surface from broken coarse particle, interface between particle and matrix and grain boundary. The micro-crack initiation has the characteristics of randomness and diversity and the main crack is generally formed on the surface of the specimen. Fatigue crack propagation path may deviate from the direction with the max loading and appear in the form of deflection, fork, convergences and bridge connectivity. This can be attributed to the influence of microstructural characteristics, which also affect the fatigue crack propagation direction and growth rate.

**Key words:** high strength aluminum alloy; crack propagation; crack deflection; bridge connectivity

**1. Introduction**

B93T4 high strength aluminum alloy in this study can match with the 7075 (United States), widely applied in aerospace, military, transportation and other fields due to the characteristics of low density, high strength and hardness and good processability, which has become one of the

most important structure materials in these fields [1-2].

As a typical high strength forging aluminum alloy, B93пч alloy composition do not contain Mn, Cr, Zr and other similar elements causing extrusion effect, because of this, its performance is highly uniform in all directions and the quenching strength loss is insignificant. At the same time, in order to improve the mechanical properties and corrosion resistance of the alloy, the content of Fe is generally controlled at about 0.2%, while the content of Si is controlled below 0.2%.

Anti-fatigue performance is increasingly required as structural components are generally subjected to fatigue cyclic loadings. For B93пч alloy, its fatigue behaviour and the underpinning micromechanism such as crack initiation and propagation have become the research focus recently [3-5]. In recent decades, great progress has been achieved in understanding of the high cycle fatigue behavior of high strength aluminum alloys [6-7], and micro-crack initiation and propagation mechanisms [8-9]. Application of fracture mechanic in crack propagation characteristics [10] has been regarded as another advantage. The effect of micro texture on short fatigue crack growth in high strength aluminum alloy Al-Li8090 and AA 2026 were studied by Zhai et al. [11] and the key factor of controlling short fatigue crack growth was the crack plane torsion and the inclination angle at the grain boundary. A larger torsion angle provided increased crack growth resistance at grain boundaries. The Al-Zn-Mg-Cu alloy fatigue crack propagation under different pre tension conditions were studied by Kassim S.Al-Rubaie et al. [12] It was found that the fracture toughness of the alloy decreased by increasing the pre tension times. The fatigue damage micromechanism of 7075-T651 aluminum alloy rolling plate were studied by Y.Xue et al. [13]

In order to explore the effect mechanism of grain, grain boundary, grain orientation and other

microstructures on fatigue crack initiation and propagation behavior, the microstructure evolution of the alloy under the cyclic loading condition with different times was systematically studied in this paper.

## 2. Experimental materials and methods

B93 aluminum high strength aluminum alloy forging was used as the test material, the chemical composition (mass fraction, %) is Zn6.5-7.3Mg1.6-2.2Cu0.8-1.2Fe0.2-0.4Si<0.2, Al margin. The alloy forging was quenched and cooled after heat preservation at 470°C for 60 minute, 2% pre stretch was carried out to release the quenching residual stress, and then 115 °C/8h+165°C/16h double stage aging treatment was carried out .

Fatigue loading testing was conducted at room temperature with a MTS810 fatigue testing machine and the maximum load was 300Mpa with sine-wave loading way of 10Hz and a stress ratio of  $R=0.1$ . Fatigue testing specimen was machined from an 8mm thickness plate of B93 aluminum alloy according to 26077-2010 GB/T standard and the specific size and processing schematic diagram was shown in Fig. 1.

The intermediate parallel section of the specimen was treated with water polishing firstly, the fatigue loading with different cyclic times was carried out after corroding with 2mL HF, 3mL HCL, 5mL HNO<sub>3</sub>, 190mL H<sub>2</sub>O mixed acid, and then the metallographic microstructure observation was carried out after unloading. The specimen was unloaded after  $1 \times 10^2$ ,  $1 \times 10^3$ ,  $1 \times 10^4$  times fatigue cyclic loading, respectively. The specimen from the intermediate deformation area was further grinded, two jet tinning, perforated, then carrying on the transmission microstructure observation. The scanning morphology of crack propagation with different cyclic times was observed by using the loading-unloading observation-loading-unloading observation forms, and

carrying on the process until the specimen fractured. Considering the maximum range of SEM equipment lofting platform, fatigue specimen of SEM observation were machined into special geometry based on *GB/T 26077-2010* standard and the specimen plate thickness is 3mm, the specimen length is 60mm.

### 3. Results and discussion

The metallographic microstructures under cyclic loadings with different durations are shown in Fig. 2. It can be seen that the amount of slip lines increases and the distance between the slip lines also increases with the increase of cycles times  $N$ . The slippage appear in only a few grains (Fig. 2a) after  $1 \times 10^3$  times cycles, the number and distance of slip lines increase and the degree of slip is deeper after  $5 \times 10^3$  times cycles (Fig. 2b). It also can be observed that slip bands can be observed only in the local region of high stress or strain. Slippage occurs only within a single grain, and the slip lines direction of the adjacent grains is not consistent, this is caused by the different orientation of the individual grain.

Slip bands extrusion and concave can be observed on the grain boundaries of specimen surface (Fig.2c-d) by increasing cyclic loading times. For a weaker grain boundaries strength, the stress required to grow the crack through the grain boundaries is much lower than that through the slip bands in the grains. As a result, fatigue crack initiates more easily from the grain boundaries (Fig. 2e-f).

The SEM morphology on fatigue specimen surface after cyclic loading is shown in Fig. 3. The micro-crack initiates in the middle disconnection of the particles (including the broken particle produced during processing), particle and matrix interface, grain boundary, etc. and further propagated to be the main crack by competing in the subsequent cyclic loading process.

Further analysis of broken particles by EDS indicates the coarse bulk phase is mainly  $\text{Al}_6(\text{CuFe})$ , as shown in Fig. 3e. Due to the poor compatibility between the coarse particles and the surrounding matrix, it is easy for crack to initiate at the interface.

The dislocation evolution of alloy fatigue specimen with different cyclic loading times under the transmission electron microscope was investigated, as shown in Fig. 4. All images were taken from Al (100) crystal plane. The corresponding plane electron diffraction is shown in the insert.

In Fig. 4, with the increase of cyclic loading times  $N$ , the number and density of the dislocation lines are increased gradually and the slip direction of the dislocation line is roughly the same as that of the cyclic loading stress (as the arrows show in Fig. 4). At the beginning of the cyclic loading, the dislocation density is relatively low and a small amount of dislocation bands can be randomly observed, with a large interdistance, Fig. 4a-b. With the increase of cycles, the dislocations are converged to bundles and dislocation bands are formed in the favorable dislocation slip directions. A small amount of random dislocations are distributed among the dislocation bands. In addition, some cross dislocations can be observed, as a result of the multiple slip systems, as shown in Fig. 4c-d. With the cycles of  $1 \times 10^4$ , the dislocation bands are more significant and the distance between the dislocation bands is further reduced, but the dislocation density of the dislocation bands are increased rapidly, as shown in Fig. 4e-f. At the same time, network-like dislocation lines are formed along a number of favorable directions.

It is possible for dislocations to encounter with fine precipitates or grain boundaries. Consequently, slippage is blocked and aggregated, thus leading to piling up in the vicinity of the sediments or grain boundaries. The location where a large number of dislocations aggregate may become the initiation sites for fatigue cracks, as shown in Fig. 5.

It is found that the fatigue crack generally starts on the specimen surface from different initiators and the main crack is a result of the competition among them. As shown in Fig.6, the main crack grows from the crack initiator II and the propagation from crack I is suppressed.

In general, the main crack propagates along the direction perpendicular to the loading. Due to the influence of grain boundaries, coarse impurity phase and crystalline planes, crack propagation can occur along different directions, following the path with the lowest resistance, as shown in Fig. 7.

The local area at the crack tip (Fig. 6b) was further examined at a higher magnification, Fig. 7. The fatigue crack is deflected several times, and some deflection angles are close to 90 degrees. When the crack propagates to next grain interface, if the misorientation between the two adjacent is very large, the propagation of the effective slip surface into the next grain becomes difficult, and the crack will tend to move along the grain boundary and continue to move forward. Crystal, due to the face centered cubic structure of aluminum alloy, the primary slip system is  $\{111\}\langle 110\rangle$ , 12 equivalent (111) faces, when cracks propagate along a plurality of mutually non parallel  $\{111\}$  surfaces in the grain, cracks propagate along the sliding surface which is most beneficial to the propagation, and thus the deflection degree is different.

After  $5 \times 10^5$  times cyclic loading, the crack growth rate is faster and faster and the crack opening degree is greater. The plastic deformation zone of the crack tip is very obvious due to the stress concentration, as the dotted circle shows in Fig. 8a. But also some branching cracks can be observed, which further illustrates fatigue cracks can select path arbitrarily in propagation process, but only the easiest propagation direction eventually become the main crack path selection, as the black arrow referred to in Fig. 8a.



The observation of plastic zone at the crack tip suggests the fatigue crack should propagate along the right obliquely downward direction. In contrast, instead of propagating along the direction anticipated, it shifts and merges with micro-crack after 500N loading, which indicates that the tiny secondary crack at the crack tip plays a role in bridging connectivity in coalescence process with the main crack, thereby speeding up the main crack propagation process. Also we can find, after 500N cyclic loadings, the main crack continues to propagate and bridge with the micro-crack ahead, but previous some cracks bifurcate or other micro cracks are inhibited, not further propagate, as dotted circles maker in Fig.8b.

The interactive relationship morphology between fatigue crack and the coarse particles in the propagation process is shown in Fig. 9a. It can be found from EDS analysis results in Fig. 9b, these coarse residual phase are mainly T phase (AlZnMgCu). When the crack pass by the position of the residual phase particles, as residual phase particles are relatively hard, cracks cannot penetrate particles, only propagating forward along the particles and matrix debonding interface position, forming propagation morphology of crack round the residual phase particles. At the same time, residual phase particles are used as the link points in the course of fatigue crack propagation, functioning bridge, changing crack propagation direction and increasing the fatigue crack propagation rate, as the white arrow shown in Fig. 9a.

As is shown in Fig. 3, many small cracks appear in the early stage of fatigue cyclic loading , although these cracks have not formed the main crack and propagated forward, these cracks may confluence and bridge with the main crack in the subsequent sustained loading process, thus greatly accelerating cracks propagation rate. It can be found by contrasting with Fig. 3d, the fine crack has been formed and been in the main direction of the main crack propagation path after

$1 \times 10^4$  times cyclic loading, as the black arrow shows in Fig. 9. When the cyclic times reach  $1 \times 10^5$  times, the main crack propagates forward to this position, in order to select the propagation path which is more conducive to fatigue crack propagation, the main crack even appear two vertical deflection, so that it is convenient to join with the fine crack, which accelerates the fatigue crack propagation process, as white dotted box shows in Fig. 9.

Fig. 10 shows the scanning morphology observation results for alloy fatigue specimen after  $2 \times 10^5$  times cyclic loading. From the figure we can find that when cracks propagation encounter grain boundaries, debonding pits, broken particles, fine cracks initiating on these positions may sink into the ring, namely cracks may not pass through the grain inside, but confluence with these fine cracks divided into multi path propagation along the grain boundaries and other interfaces, then synthesized one to continue to propagate forward. These grain boundaries, pits and broken particles play a significant bridging role in the path of crack propagation, which greatly accelerate the fatigue crack growth rate.

If the micro misorientation in adjacent intercrystalline is insignificant, the effective slip surface of the front grain is easier for crack propagation, then the fatigue crack will choose to cross the grain boundaries and move forward to propagate in the next grain. The white dotted line in Fig. 9 is further amplified and observed, and the micro morphology at crack tip is obtained in Fig. 11. We can see that when the crack propagates along the boundaries to a three fork grain boundaries, the crack can choose to propagate along with the two grain boundary interfaces of the next grain, also can be selected to propagate in the grain inner. Crack propagation path deflect large angle (about 120 degrees) due to the poor strain compatibility around the grain boundaries, which will reduce the effective driving force of crack propagation, the propagation will be blocked

by a large degree. And if the micro misorientations in adjacent intercrystalline is insignificant, the effective slip system of the next grain required start energy is very low, then crack can easily enter a grain forward transgranular propagation, which need to deflect at a very small angle as shown in Fig. 11b.

The fracture morphology of fatigue specimen after about  $3 \times 10^6$  times cyclic loading is shown in Fig. 12. The deflection, bifurcation and large angle deflection of fatigue crack in the propagated path selection can be observed in Fig. 12.

A lot of fine cliffs are shown in the fracture surface in the early stage of crack propagation which is arranged in parallel to crack propagation direction. At high magnification, ladder appearance pattern in the grain interior is formed in the tiny cliffs, which indicating that the crack tip in the crack propagation process has lateral deflection slip (Fig. 12a-b). Fig. 12c shows the morphology observation results of the fatigue crack's stable propagation period of the specimen fracture surface. The white arrow shows the direction of fatigue crack propagation. It can be seen from the figure, fatigue striation spacing are different on both sides of the grain boundaries and the directions are not consistent, which indicates that the fatigue crack propagation path deflection occurs at the crossing of the grain boundaries, and the propagation rate is also different in the adjacent two grains. When cracks growth passes through the grain boundaries, the grain boundaries may accelerate or delay the crack propagation. This is because there is a certain angle between the effective slip surface of two adjacent grains, and the size of the included angle determines the role of grain boundaries. According to the deflection-torsion model from Jian et al [14], the larger the angle, the greater the driving force for crack deflection, the more difficult the crack deflection, on the contrary, it is easier for crack to accelerate the expansion in the next grain.

The location of the crack source for smooth fatigue specimen is random and non single, micro-cracks can form on the specimen surface, grain boundaries, debonding interface between particles and matrix and broken particles, etc. Multiple micro-cracks formed propagate into the main crack through competition, and when the main crack formed, the other cracks will terminate the propagation. When the main crack is in the expansion stage, some coarse particles with high strength are in poor coordination with the matrix during cyclic stress loading, resulting in debonding with the matrix, and even cracking, resulting in a large number of tiny secondary cracks around them. As the crack continues to propagate, if residual phase, debonding pits exist in the crack front along the direction of the maximum shear stress, which play a role of bridging connection in the crack propagation process, tiny secondary cracks will be merged with the main crack, thus speeding up the expansion process of the main crack, causing the deflection of the main crack at a certain degree. At the same time, as the test material is forged aluminum alloy, some coarse residual phase particles also have their own cracking phenomenon in the process of machining, which provides a great convenience for the formation of tiny cracks.

As the control precision of alloy ingot composition, metallurgical quality and uniformity is limited in industrial production, it is inevitable that some coarse residual phase particles exist in the alloy materials. Due to the large size of these residual phases, the strengthening effect of the alloy is not promoted, but it is easy to become the place of crack initiation and propagation due to the stress concentration when the external force is applied. And which will have a harmful effect on the fatigue property and the stress corrosion resistance of alloy. In addition, the mechanical properties of aluminum alloy are also determined by the microstructure characteristics of the grain, grain boundary, second phase and dislocation, etc. In this study, the microstructure of fatigue

behavior of the alloy is observed and analyzed, and also analyze the microstructure factors of fatigue crack initiation and propagation behavior. In this way we can take different heat treatment technology to guide and control the microstructure of the alloy in production practice, so as to achieve the purpose of prolonging life for alloy material and improve its various mechanical properties.

#### 4. Conclusions

1) Fatigue micro-crack initiation is random and varied and the main crack generally initiates on the surface of the specimen. Fatigue micro-crack is usually easy to initiate on the surface from coarse particle caused in the thermal processing, debonding hard phase particles of the poor strain coordination with the surrounding matrix and the stress concentration areas caused by the dislocation pile-up around grain boundary or precipitate. These micro-cracks cannot be the main crack in the subsequent competition expansion process, but in the process of propagation path selection, the deflection, fork, convergence and bridge connectivity of propagation path can be attributed to the micro structural characteristics such as grain boundary and second phase, which affect the fatigue propagation direction and rate as well.

2) Fatigue crack propagation of B93пч alloy is divided into intergranular propagation and transgranular propagation, the choice of intergranular or transgranular propagation is mainly dominated by the direction of stress loading, at the same time, it will be affected by the micro structures of grain boundary, grain micro orientation, etc. If the micro orientation difference between adjacent grains on the crack growth path is insignificant, the effective slip surface of the front grain is easier to cause crack growth, then the fatigue crack will choose to cross the grain boundaries and choose transgranular propagation in the next grain size at a very small angle.

**Acknowledgements**

This work was financially supported by the National Natural Science Foundation of China (51301065) and Natural Science Foundation of Hunan Province (14JJ7067).

**References**

- [1] H.C.Fang, K.H.Chen, H.Chao, et al. *Mater. Sci. Eng. Powder. Metall.* 6(2009) 351.
- [2] T.Warner. *Mater. Sci. Forum.* 2(2006) 1271.
- [3] C.F.Ding, J.Z.Liu, X.R.Wu. *J.Aeronautical Mater.* 6(2005) 11.
- [4] H.G.Jian, F.Jiang, K.Wen, et al. *Trans. Nonferrous Met. Soc. China.* 5(2009) 1031.
- [5] Y.Y.Chen, Z.Q.Zheng, B.Cai, et al. *Rare Meter Mat Eng.* 11(2011) 1926.
- [6] S.Suresh. *Fatigue of Materials.* London: Cambridge University Press, 1998.
- [7] M.Lewandowska, J.Mizera, J.W.Wyrzykowski. *Mater Charct.* 45(2000) 195.
- [8] Z,Q.Zheng, X.X.Sun, Y.Y.Chen, et al. *Rare Meter Mat Eng.* 6(2010) 975.
- [9] N.Kamp, N.Cao. *Int. J. Fatigue.* 29(2007) 869.
- [10] M.Oja, K.S.Ravi Chandran, R.G.Tryon. *Int. J. Fatigue.* 3(2010) 551.
- [11] T.Zhai, A.J.Wilkinson, J.W.Martin. *Acta Mater.* 48(2000) 4917.
- [12] K.S. Al-Rubaie, E.K.L. Barroso. *Int. J. Fatigue.* 28(2006) 934.
- [13] Y.Xue, H.E. Kadir, M.F.Horstemeyer. *Acta Mater.* 55(2007) 1975.
- [14] H.G.Jian, F.Jiang,L.L.Wei, et al. *Mater. Sci. Eng., A.* 527(2010) 5879-5882.

**Figures**

Fig. 1 Processing diagram of fatigue testing specimen (unit: mm)

Fig. 2 Observation of slip bands on the specimen surface under cyclic loading

a)  $N=1\times 10^3$ ; b)  $N=5\times 10^3$ ; c-d)  $N=1\times 10^4$ ; e-f)  $N=1\times 10^5$

Fig. 3 Initiation of fatigue crack  $N=1\times 10^4$

Fig. 4 Dislocation structure under different cyclic times

a-b)  $N=1\times 10^2$ ; c-d)  $N=1\times 10^3$ ; e-f)  $N=1\times 10^4$

Fig. 5 Dislocation structure of fatigue specimen after cyclic loading  $N=1\times 10^4$

Fig. 6 Observation of fatigue crack source  $N=1\times 10^5$

Fig. 7 Morphology of fatigue crack propagation  $N=1\times 10^5$

Fig. 8 Bridge connectivity of crack propagation  $N=5\times 10^5$

Fig. 9 Bridge effect of particles on crack propagation  $N=1\times 10^5$

Fig. 10 Fatigue crack lane propagation and confluence  $N=2\times 10^5$

Fig. 11 Transgranular propagation of fatigue crack  $N=1\times 10^5$

Fig. 12 Fracture morphology of fatigue specimen  $N=3\times 10^6$

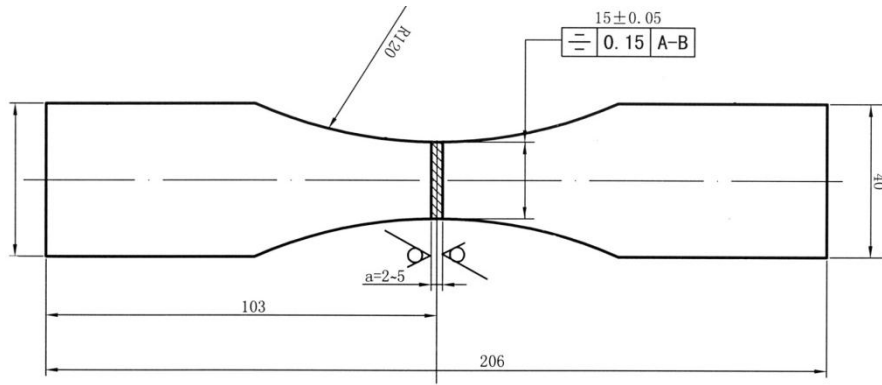


Fig. 1 Processing diagram of fatigue testing specimen (unit: mm)

Accepted manuscript



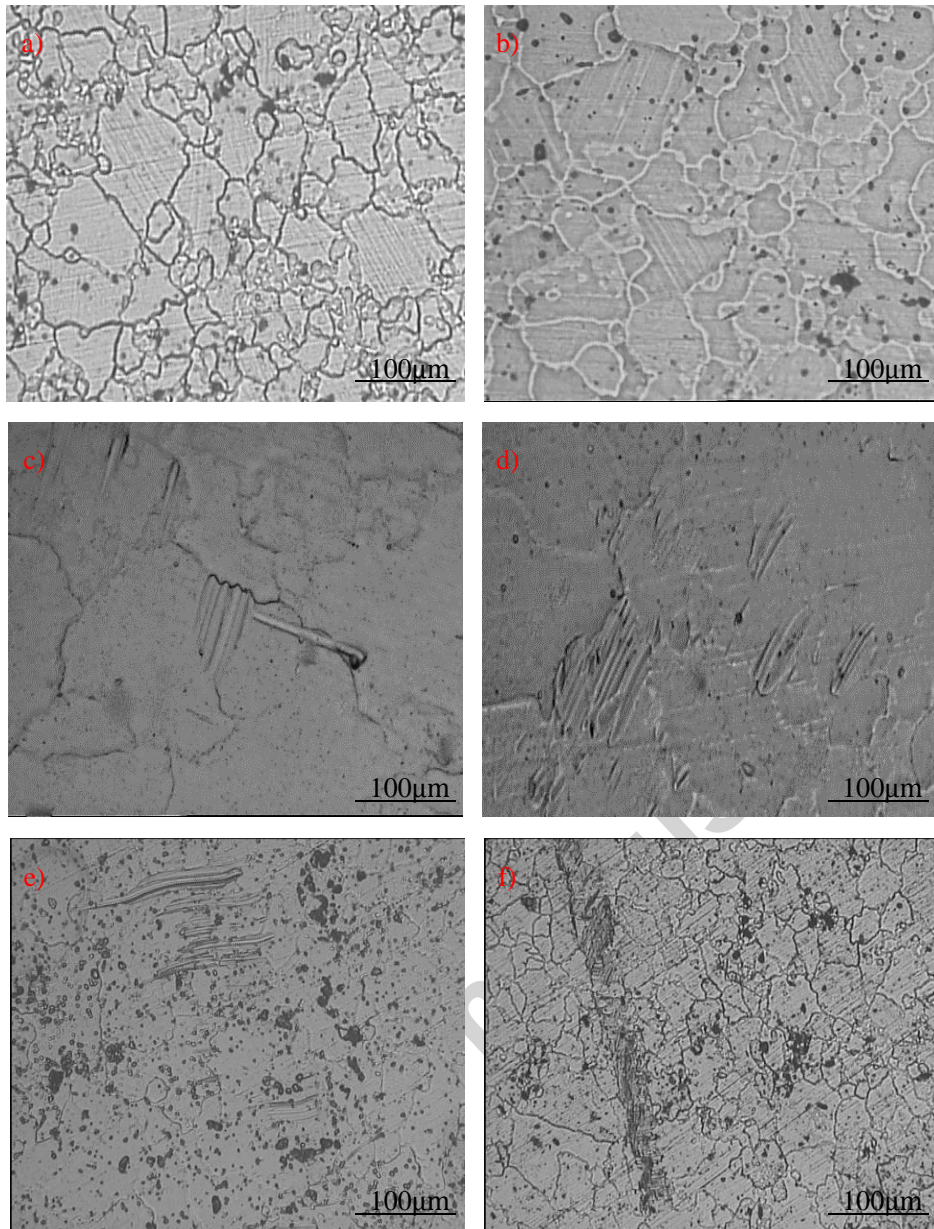
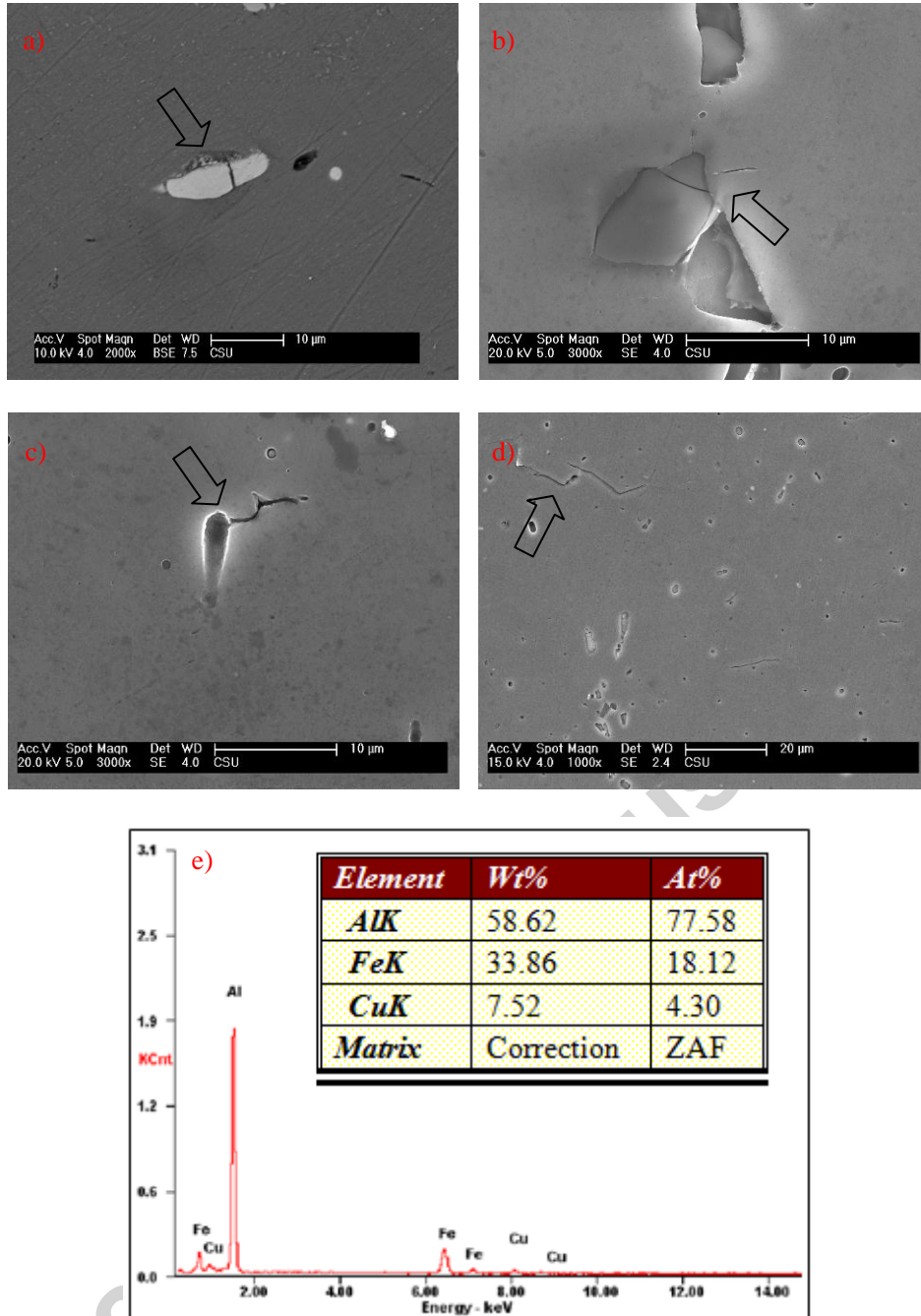


Fig. 2 Observation of slip bands on the specimen surface under cyclic loading

a)  $N=1 \times 10^3$ ; b)  $N=5 \times 10^3$ ; c-d)  $N=1 \times 10^4$ ; e-f)  $N=1 \times 10^5$

Fig. 3 Initiation of fatigue crack  $N=1 \times 10^4$

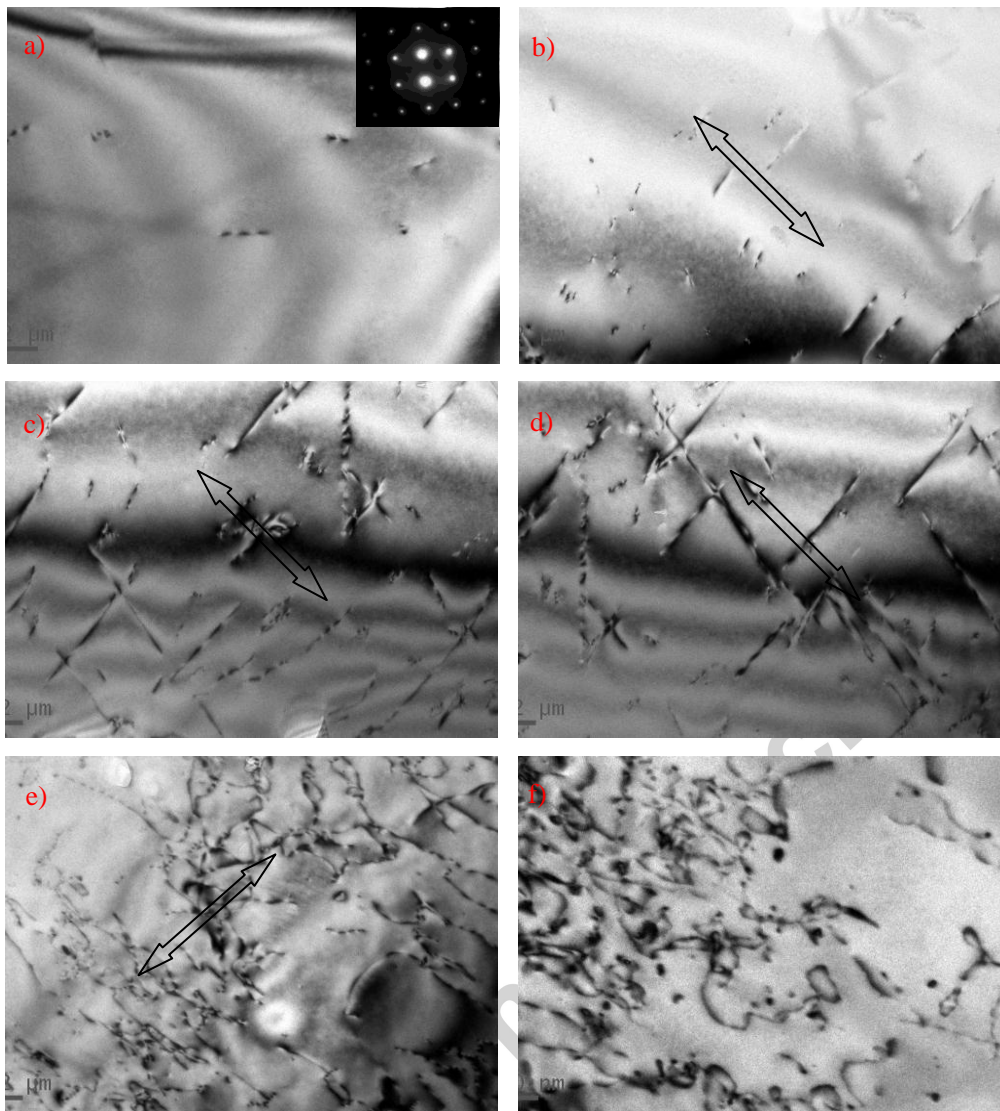


Fig. 4 Dislocation structure under different cycle times

a-b)  $N=1 \times 10^2$ ; c-d)  $N=1 \times 10^3$ ; e-f)  $N=1 \times 10^4$

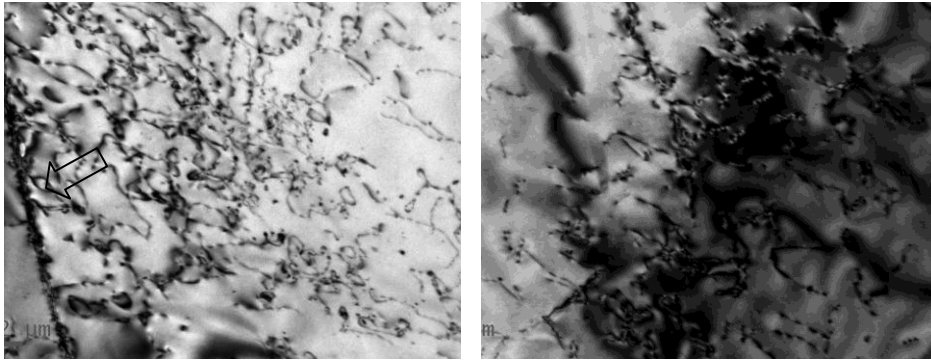


Fig. 5 Dislocation structure of fatigue specimen under cyclic loading  $N=1 \times 10^4$

Accepted manuscript



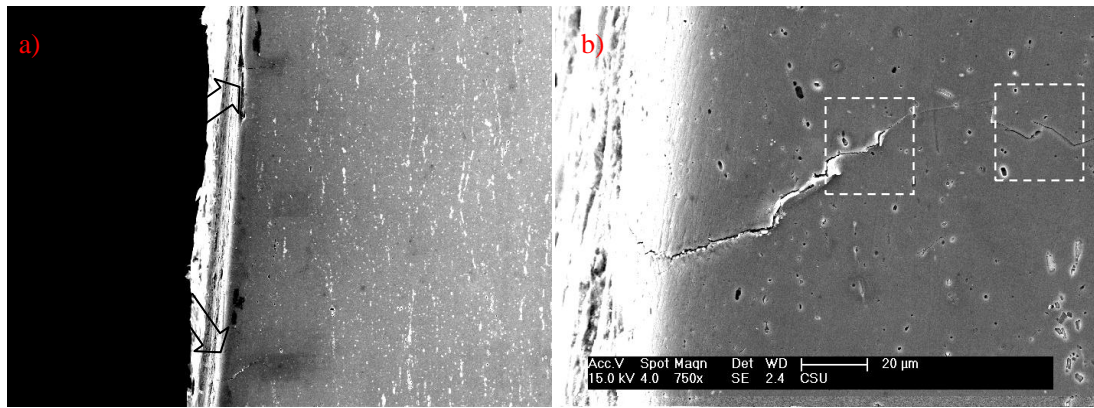


Fig.6 Observation of fatigue crack source  $N=1 \times 10^5$

Accepted manuscript

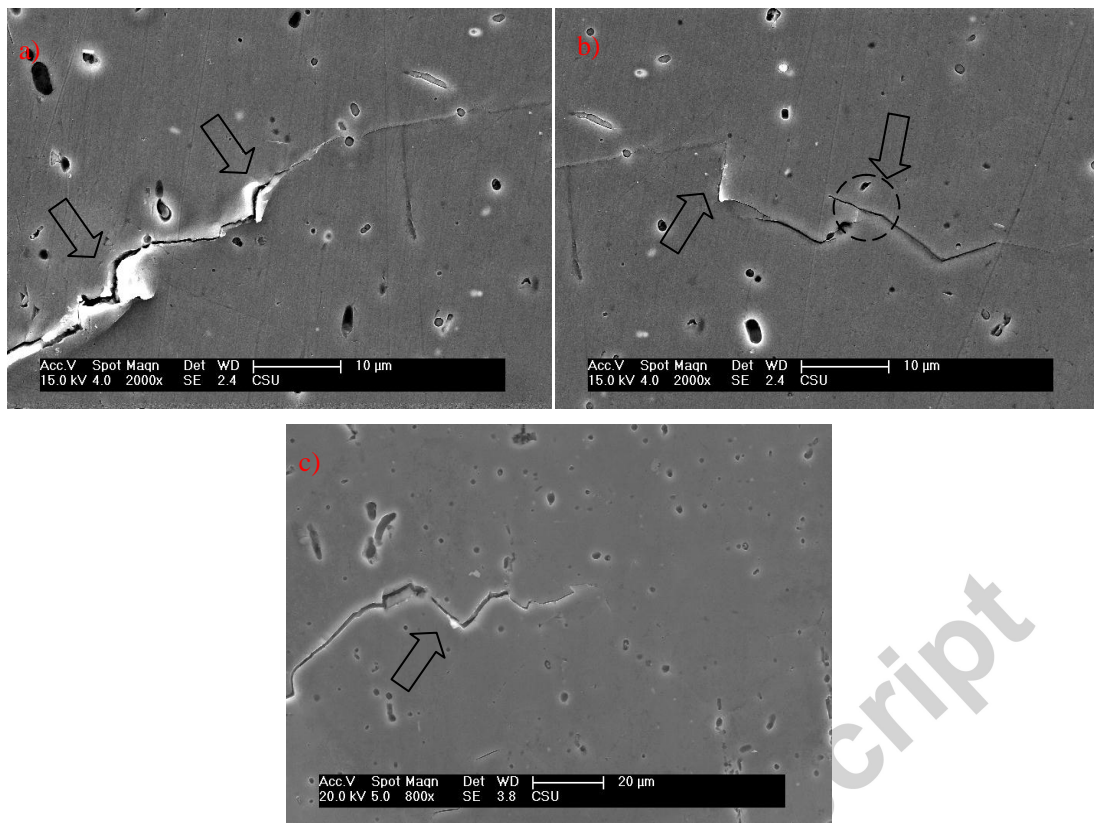


Fig. 7 Morphology of fatigue crack propagation  $N=1 \times 10^5$

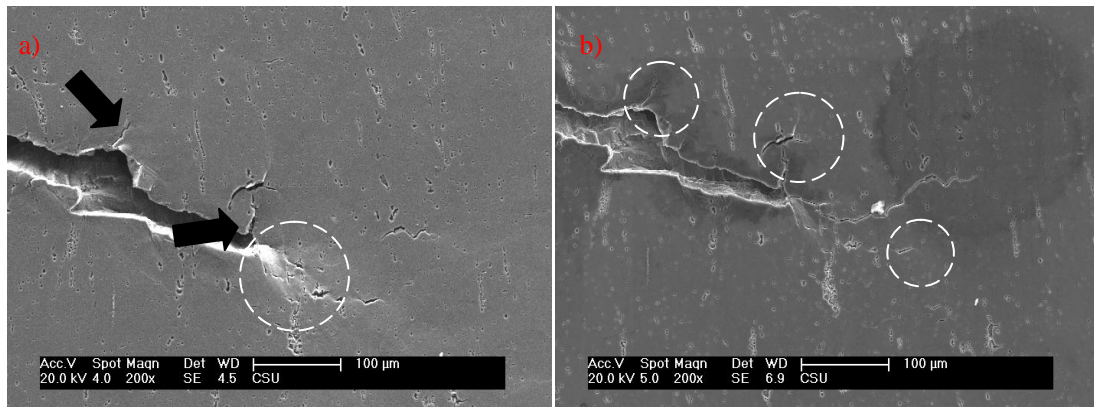


Fig. 8 Bridge connectivity of crack propagation  $N=5 \times 10^5$

Accepted manuscript

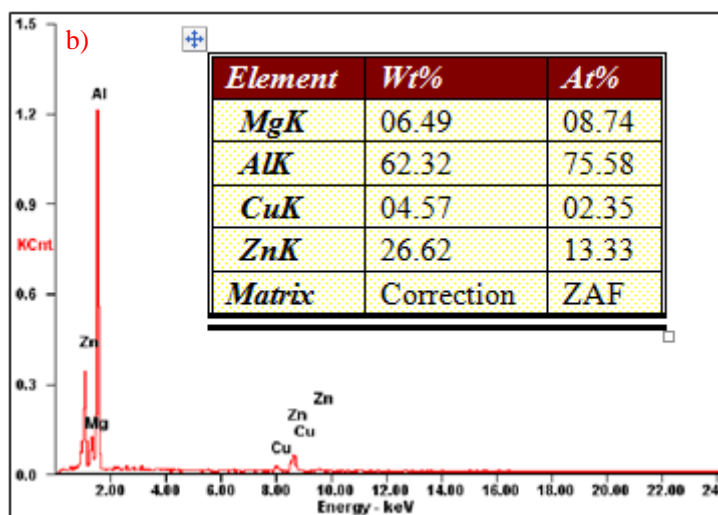
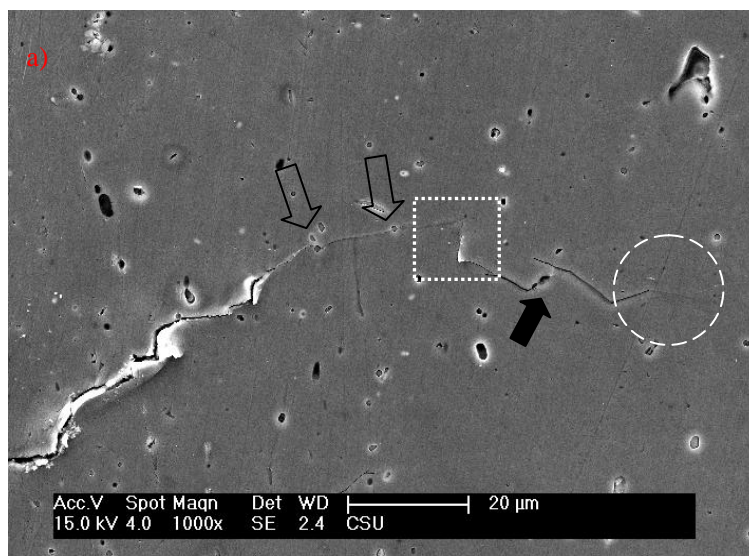


Fig .9 Bridge effect of particles on crack propagation  $N=1 \times 10^5$



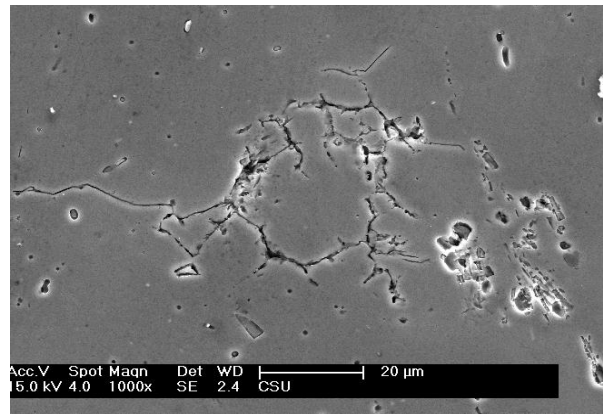


Fig. 10 Fatigue crack lane propagation and confluence  $N=2 \times 10^5$

Accepted manuscript

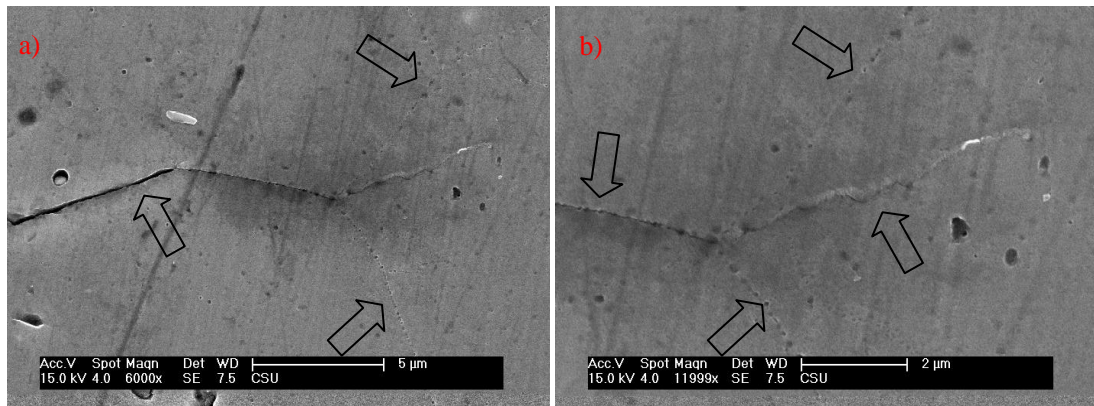


Fig. 11 Transgranular propagation of fatigue crack  $N=1 \times 10^5$

Accepted manuscript

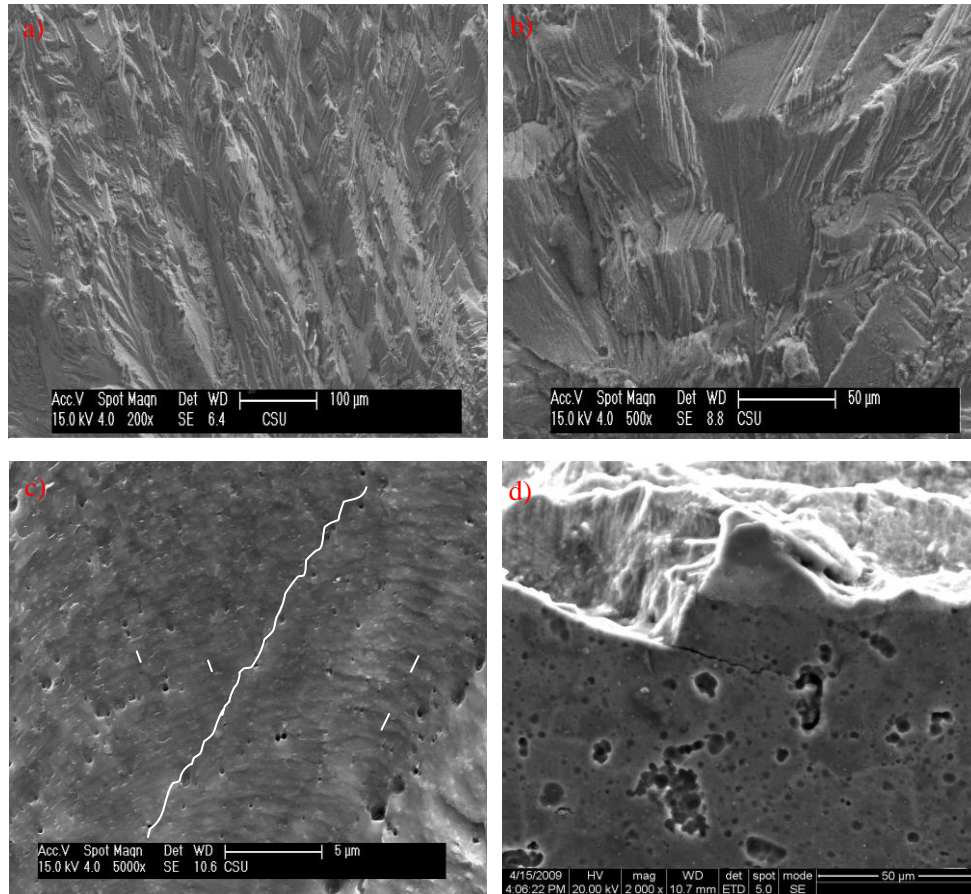


Fig.12 Fracture morphology of fatigue specimen  $N=3 \times 10^6$